1D2D Inundation Modelling using SOBEK-Rural: A Measure for Flood Risk Management

Asadusjjaman Suman[1], Farnaz Akther[2]
[1]Institute for Applied Ecology, University of Canberra,ACT-2601, Australia
[2]Software Engineering, Faculty of ESTeM, University of Canberra,ACT-2601, Australia

Abstract— *The paper presents diversion of flood water and inundation pattern in a polder with varying weir crest width and manning co-efficient. SOBEK-Rural was used to simulate 1D2D inundation pattern in the polder. Maximum weir width was found 17.5m to confine diverted flood water only in the compartment C1 with inundation depth 0.95m and downstream discharge 274 m3/sec. Water was not found on the ring dike around compartment C4 until weir width 25m. However, water was found on the western side dike of the compartment C4 with weir width 26m and water may overtop into compartment C4. To keep completely free from flood water compartment C4, it is recommended to use maximum weir width 25m. Downstream maximum discharge was found 251 m^3/sec and maximum water depth was found 1.1m, 0.1m and 0.1m for compartment C1, C2 and C3 respectively with weir width 25m.*

Manning co-efficient was found not sensitive to the maximum discharge at downstream. However, manning co-efficient was found sensitive to lag time of increasing water depth and flow velocity therefore, it was found less inundation depth and less flow velocity at a particular time with higher manning co-efficient. Spatial inundation was also found less in higher manning co-efficient and therefore it is recommended to increase manning coefficient at floodplain for effective flood risk management.

Keywords— SOBEK-Rural, Inundation Modelling, Polder, Manning Co-efficient, Flood Risk Management.

I. INTRODUCTION

About half of the natural disaster in the world is originated from the flooding problem (Vos *et al.*, 2010; Guha-Sapir *et al.*, 2004; Jonkman and Kelman, 2005). Beside this, population growth, unplanned flood plain development, rapid and unplanned urbanization increases flood risk across the globe (De Moel *et al.*, 2011; and Taylor *et al.*, 2013). Investigation of inundation pattern, before development of an area is worth to reduce flood risk of that area. The Overland Flow (2D) module of SOBEK-Rural (Deltares Systems, 2014) is designed to calculate 2D flooding scenarios. The module is fully integrated with the 1D-FLOW module for accurate flooding simulation. The hydrodynamic simulation engine underneath is based upon the complete Saint Venant Equations (Feng et al., 2006; Xu et al., 2012). It can simulate steep fronts, wetting and drying processes and sub critical (Kesserwani et al., 2008) and supercritical flow (Mustaffa et al., 2013). In addition the experience of this model is used to flood risk management for real life problem.

II. PROBLEM DESCRIPTION

It is shown in Fig. 1 the map of the 1D/2D network from Dordrecht, The Netherlands. The river flows from South East to North West is connected to the inundation area (2D grid) by a flood relief channel, which is controlled by a weir. Fig. 2 shows detail of flood relief channel.

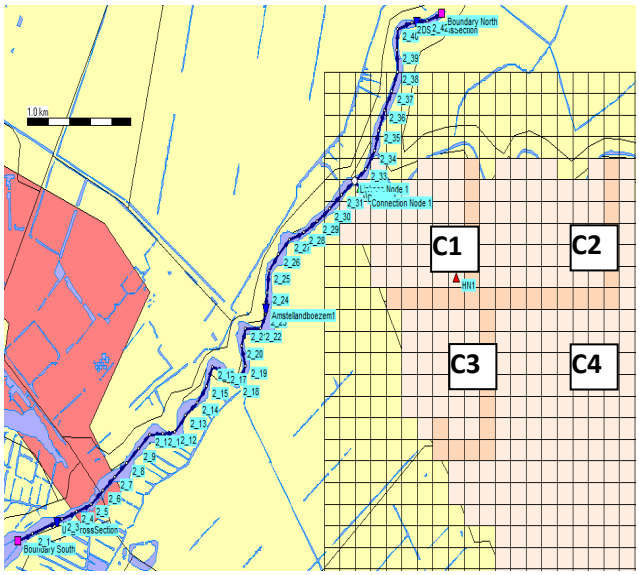

Fig. 1. 1D/2D network and four compartments of the inundation area

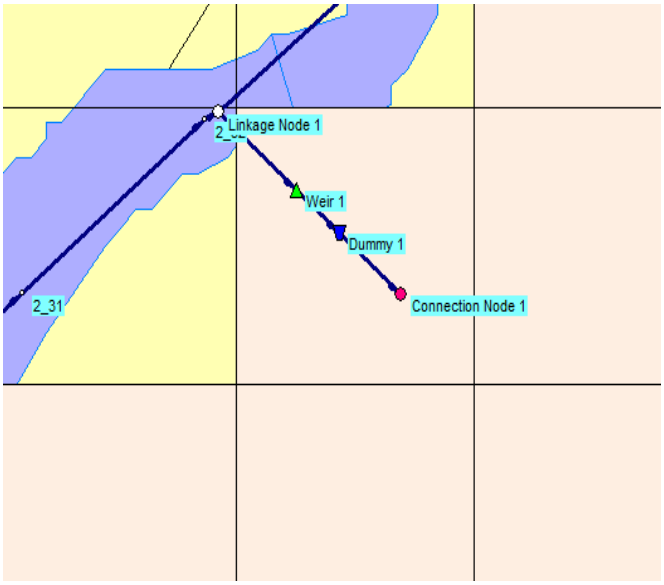

Fig 2: A detail of the flood relief *channel and weir*

The inundation area is a polder (Bouwer et al., 2010; van Manen and Brinkhuis, 2005) that is divided in different compartments C1, C2, C3 and C4. The controlled inundation of the polder can be necessary in order to prevent dikes (Stanczak and Oumeraci, 2011; Vorogushyn et al., 2011) from breaking at some other point in the channel, causing economic damage and possibly loss of human lives (Jonkman et al., 2009). Hence, the "cost" of this flood relief structure is the inundation of the polder, while the "benefit" is the reduction of the downstream river discharge. It is recommended to keep compartment C4 free from flood water and preferably C2 and C3 less flood water.

III. METHODOLOGY

SOBEK-Rural is developed by Deltares (Deltares Systems, 2014) is capable for modelling irrigation & drainage systems, natural streams in lowlands and hilly areas. Applications are typically related to optimizing flood control, irrigation, canal automation, reservoir operation, agricultural production, and water quality control. SOBEK-Rural can also answer questions about increased pollution loads in response to growing urbanisation.

SOBEK-Rural offers the support If needed for effective planning, design and operation of new and existing water systems. The software calculates the flow in simple or complex channel networks. It is possible to define all types of boundary conditions (Prange and Gerdes, 2006; Prario et al., 2011), as well as define lateral inflow and outflow using time series or standard formula. For more detail, the rainfall run-off process of urban areas and various types of unpaved areas can be modelled, taking into account land use, the unsaturated zone, groundwater, capillary rise and the interaction with water levels in open channels.

Base model was developed with available hydrologic & hydrodynamic data, DEM of study area, and necessary field data. After developing the base model, model was run for different scenario. Model output and necessary Fig.s area describe in following sections.

IV. RESULT AND DISCUSSION

Fig. 3 shows the hydrograph at upstream, middle section and downstream at base scenario with weir width of 12 m. The discharge at downstream section was found about 300 m^3/sec.

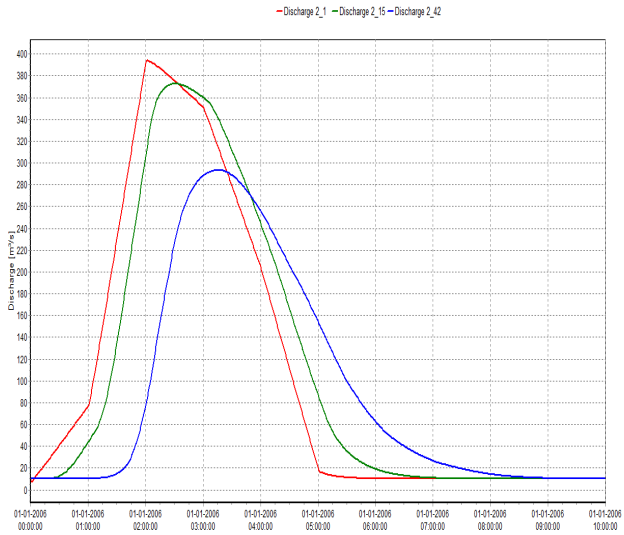

Fig. 3: Hydrograph at upstream, middle section and downstream at base scenario with weir width 12 m

Fig. 4 shows, inundation depth in compartment C1. Fig. 5 shows the inundation area for base scenario with weir width 12 m. It was found that only compartment C1 was inundated.

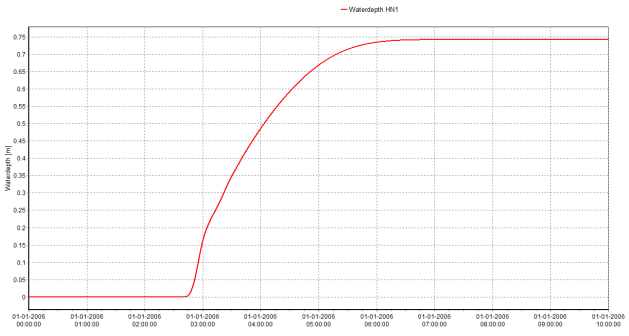

Fig. 4: Inundation depth at base scenario

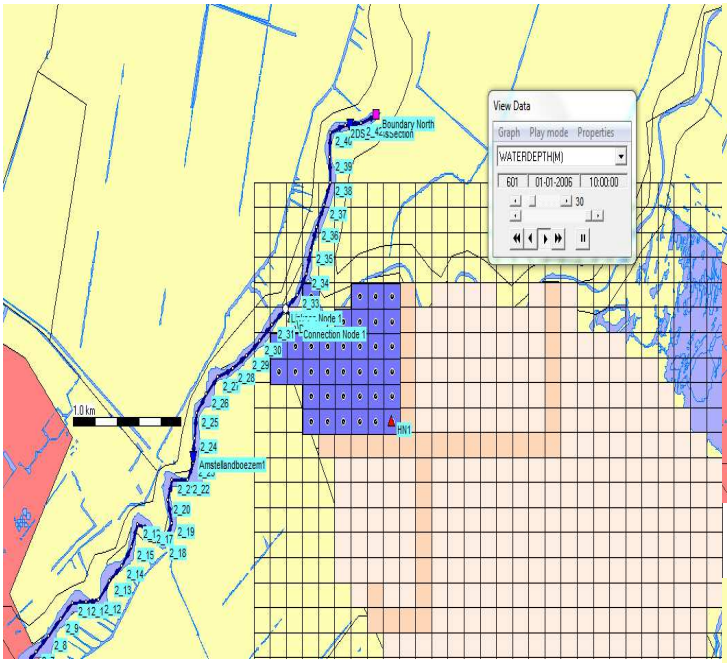

Fig. 5: Inundated area at base scenario with weir width 12m

It was found the optimum width of weir is 17.5m where the inundation was confined within only compartment C1. At different model run, it shows when weir width was increased the depth of inundation was also increased in compartment C1 and on the other hand the peak discharge was decreased at downstream. At optimum condition with weir width 17.5 m the peak discharge at downstream was found about 274 m^3/sec whether at base scenario it was about 300 m^3/sec.

To find the optimum solution, a historical node at south west corner of compartment C1 was placed. By which it was possible to check the depth of inundation at every model run with increasing width of weir. At weir width 17.5m, it was found the depth of flood water is about 0.95 m. The height of ring dike is 1.0 m so it is recommended to use maximum weir width of 17.5 m while all flood water will confine in compart C1 only.

It was recommended to keep compartment C4 free from flood water, while preferably less flood water into the compartment C2 and C3. The model was iteratively run until found water on dike. Until weir width 25m, we did not fine water on dike around compartment C4(Fig. 6). However, at weir width 26m, water was found on dike adjacent to the compartment C4 (Fig. 7). At this case water may overtop into compartment C4. So, it is recommended to use maximum weir width 25m to keep completely free C4 from flood water. With this weir width, maximum downstream discharge found 251 m^3/sec while it was reduced 49 m^3/sec from base scenario.

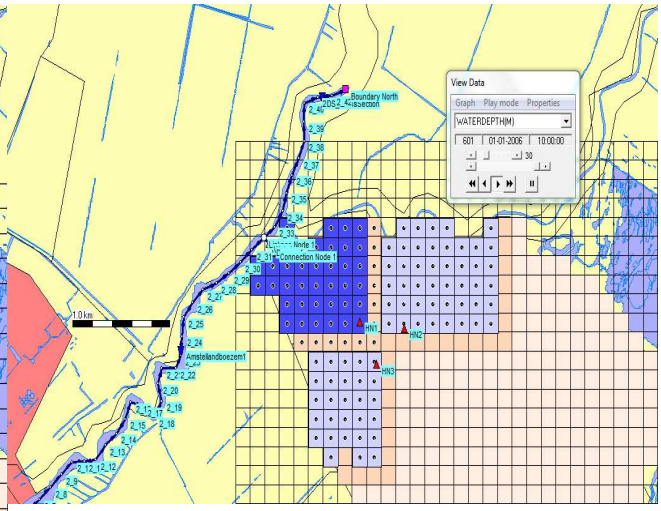

Fig. 6: Inundated area with weir width 25 m

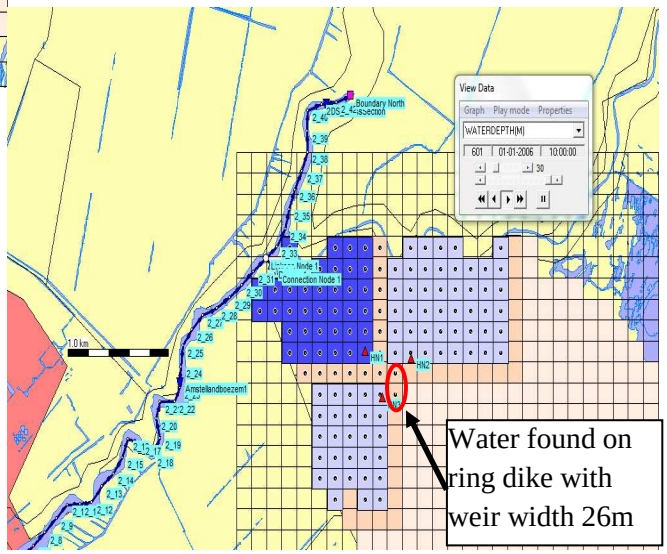

Fig. 7: Inundated area with weir width 26 m

Fig. 8 shows water depth with weir width 25m. Fig. 8 shows depth of water 1.1m, 0.1m and 0.1m respectively.

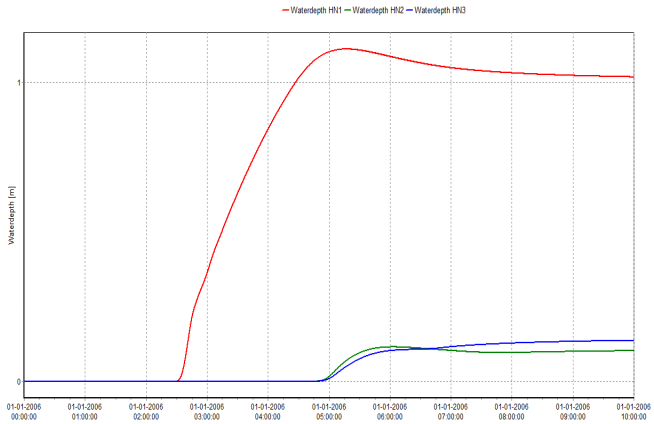

Fig. 8: Inundation depth at different compartment with weir width 25 m

Model output shows that there is no significant change in downstream hydrograph while 2D grid flood plain's Manning coefficient(Anderson et al., 2006; Ayvaz, 2013;

Noarayanan et al., 2012) changes to 0.06, 0.09 and 0.12 from the base case 0.03. At every case the peak discharge was found about 292 m^3/sec. But the total discharge at downstream might be increased for back water effect due to increasing of manning co-efficient at flood plain.

Fig. 9 and 10 Shows that the lag time (Talei and Chua, 2012) of increasing water depth is significantly changes with manning co-efficient of flood plain. From Fig. 9 it is shown the lag time of increasing depth of water is about 2hrs and 30 minutes for manning co-efficient 0.03 but for manning co-efficient 0.06 it is about 3 hrs and 30 minutes which shown in Fig. 10. From these two figures it is clear that the time difference for increasing water depth is about an hour. It is very important for flood risk management specially for evacuation during emergency period.

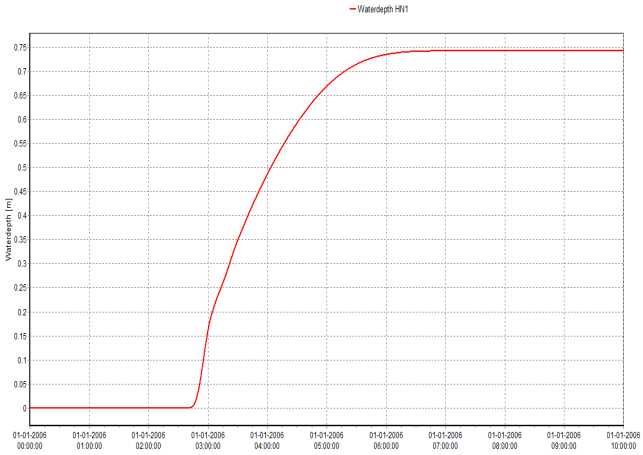

Fig. 9: Water depth at historical node 1 with manning co-efficient 0.03

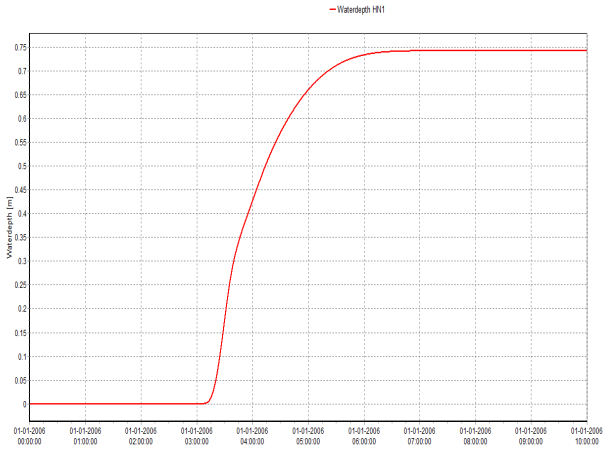

Fig. 10: Water depth at historical node 1 with manning co-efficient 0.06

Another important feature was depth of water at a particular time was varies with manning co-efficient of flood plain. It was shown that the depth of water at 4.00 AM is about 0.5 m for manning co-efficient 0.03 whether at the same time these depth are 0.35m and 0.22m for manning co-efficient 0.09 and 0.12 respectively. This is also very important for flood risk management.

Flood damage is extensively varies with flow velocity as well. Fig. 11 and 12 shows that the peak flow velocity was considerably varied with flood plain manning co-efficient. Fig. 11 shows the peak absolute flow velocity was 0.24 m/sec for manning coefficient 0.03 whether it was 0.15m/sec for the manning co-efficient 0.06 (Fig. 12) and continue decreasing with increasing of manning co-efficient.

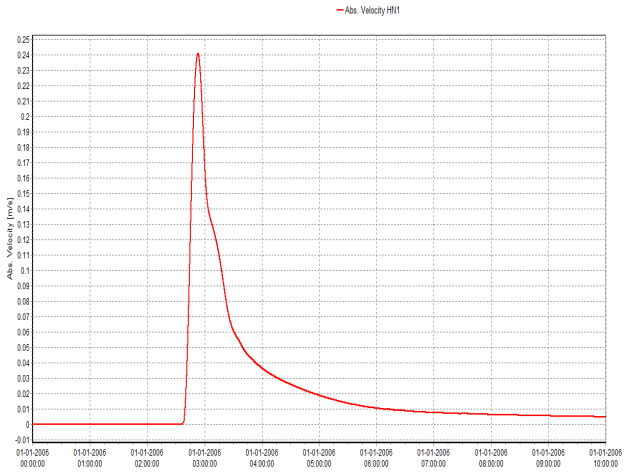

Fig. 11: Water velocity at historical node 1 with manning co-efficient 0.03

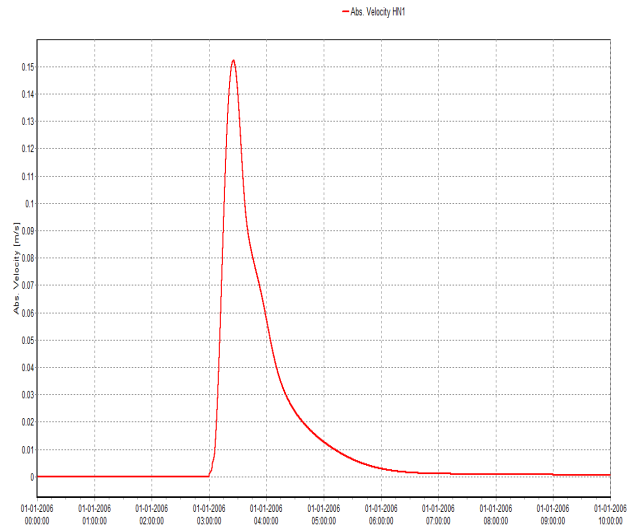

Fig. 12: Water velocity at historical node 1 with manning co-efficient 0.06

Fig. 7 and 13 shows the inundation area with different manning co-efficient. Fig. 13 shows some areas were still dry and less depth of water at compartment C2 and C3 due to higher manning co-efficient at flood plain though the width of weir is same compare to Fig. 7.

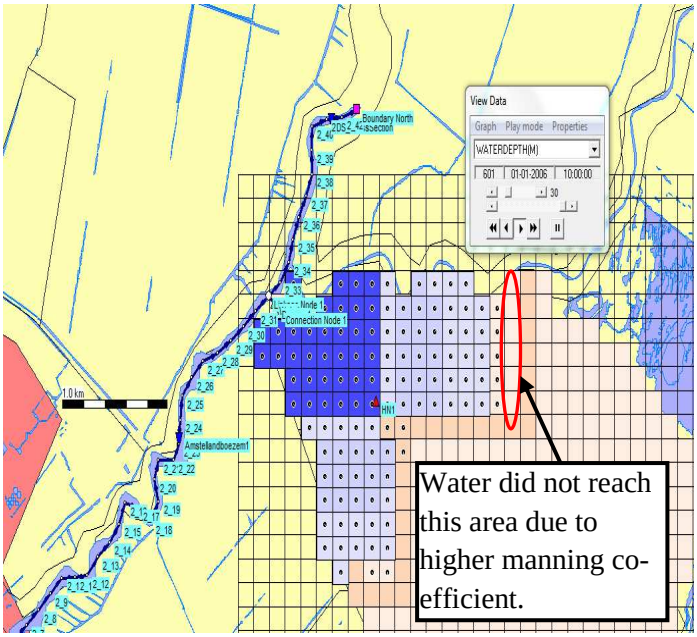

Fig. 13: Inundation area with weir width 26 m and manning co-efficient 0.12

V. CONCLUSION

The paper presents diversion of flood water and inundation pattern of a polder with varying weir crest width and manning co-efficient. Base model simulation result shows, downstream discharge 300 m^3/sec and inundation depth 0.75m with diversion channel crest width 12 m. The height of ring dike across compartment C1 is 1.00 m. The model was iterating until water depth was safe for the ring dike. Final, simulation result shows optimum width of weir 17.5m where the inundation was confined in the compartment C1 with inundation depth 0.95m and downstream discharge 274 m^3/sec.

Water was not found on the ring dike around compartment C4 until weir width 25 m. However, water was found on the western side dike of compartment C4 with weir width 26m and water may overtop into C4. To keep completely free from flood water it is recommended to use maximum weir width 25m. Downstream maximum discharge was found 251 m^3/sec and maximum water depth was found 1.1m, 0.1m and 0.1m for compartment C1, C2 and C3 respectively with weir width 25m.

Manning co-efficient was found not sensitive to the maximum discharge at downstream. However, this co-efficient was found sensitive to lag time of increasing water depth and flow velocity therefore, it was found less inundation depth and less flow velocity at a particular time with higher manning co-efficient. Spatial inundation was also found less in higher manning co-efficient and therefore it is recommended to increase manning coefficient at floodplain for effective flood risk management.

ACKNOWLEDGEMENT

We acknowledge UNESCO-IHE Institute for Water Education Delft, the Netherlands for all necessary data for the research. We also acknowledge Dr. Schalk Jan van Andel and Dr. Giuliano Di Baldassarre, UNESCO-IHE Institute for Water Education Delft, the Netherlands for their comments over the report.

REFERENCES

[1] Anderson BG, Rutherfurd ID, Western AW. 2006.An analysis of the influence of riparian vegetation on the propagation of flood waves **21**:1290–1296.

[2] Ayvaz MT. 2013. A linked simulation – optimization model for simultaneously estimating the Manning ' s surface roughness values and their parameter structures in shallow water flows. *J. Hydrol.* **500**:183–199.

[3] Bouwer LM, Bubeck P, Aerts JCJH. 2010. Changes in future flood risk due to climate and development in a Dutch polder area. *Glob. Environ. Chang.* **20**:463–471.

[4] Deltares Systems. 2014. SOBEK User Manual. Delft, the Netherlands. http://content.oss.deltares.nl/delft3d/manuals/SOBEK_User_Manual.pdf.

[5] De Moel, H., Aerts, J.C.J.H., and Koomen, E. (2011). Development of flood exposure in the Netherlands during the 20th and 21st century. *Global Environmental Change*, 21(2), 620–627. doi:10.1016/j.gloenvcha.2010.12.005

[6] Feng J-H, Cai L, Xie W-X. 2006. CWENO-type central-upwind schemes for multidimensional Saint-Venant system of shallow water equations. *Appl. Numer. Math.* **56**:1001–1017.

[7] Guha-Sapir, D., Hargitt, D. and Hoyosis, P. (2004). Thirty years of natural disasters 1974-2003: the numbers. Centre for research on the Epidemiology of Disasters, Belgium

[8] Jonkman S.N. and Kelman I. (2005). An analysis of causes and circumstances of flood disaster deaths. Disasters, 29(1), 75–97.

[9] Jonkman SN, Maaskant B, Boyd E, Levitan ML. 2009. Loss of life caused by the flooding of New Orleans after Hurricane Katrina: analysis of the relationship between flood characteristics and mortality. *Risk Anal.* **29**:676–98.

[10] Kesserwani G, Ghostine R, Vazquez J, Mosé R, Abdallah M, Ghenaim A. 2008. Simulation of subcritical flow at open-channel junction. *Adv. Water Resour.* **31**:287–297.

[11] Mustaffa Z, Madzlan N, Rasool AG. 2013. Dealing with Supercritical Flow in Culvert. *APCBEE Procedia* **5**:306–311.

[12] Noarayanan L, Murali K, Sundar V. 2012. Manning's "n" co-efficient for flexible emergent vegetation in tandem configuration. *J. Hydro-environment Res.* **6**:51–62.

[13] Prange M, Gerdes R. 2006. The role of surface freshwater flux boundary conditions in Arctic Ocean modelling. *Ocean Model.* **13**:25–43.

[14] Prario BE, Dragani W, Mediavilla DG, D'Onofrio E. 2011. Hydrodynamic numerical simulation at the mouths of the Parana and Uruguay rivers and the upper Rio de la Plata estuary: A realistic boundary condition. *Appl. Math. Model.* **35**:5265–5275.

[15] Stanczak G, Oumeraci H. 2011. Modeling sea dike breaching induced by breaking wave impact-laboratory experiments and computational model. *Coast. Eng.* **59**:28–37.

[16] Talei A, Chua LHC. 2012. Influence of lag time on event-based rainfall – runoff modeling using the data driven approach. *J. Hydrol.* **438-439**:223–233.

[17] Taylor, J., Biddulph, P., Davies, M., and Lai, K. M. (2013). Predicting the microbial exposure risks in urban floods using GIS, building simulation, and microbial models. Environment International, 51, 182–95. doi:10.1016/j.envint.2012.10.006.

[18] Van Manen SE, Brinkhuis M. 2005. Quantitative flood risk assessment for Polders. *Reliab. Eng. Syst. Saf.* **90**:229–237.

[19] Vorogushyn S, Apel H, Merz B. 2011. The impact of the uncertainty of dike breach development time on flood hazard. *Phys. Chem. Earth, Parts A/B/C* **36**:319–323.

[20] Vos, F., Rodriguez, J., Below, R. and Guha-Sapir, D.(2010). Annual Disaster statistical review 2009 - the numbers and trends. Centre for research on the Epidemiology of Disasters, Belgium

[21] Xu M, Negenborn RR, van Overloop PJ, van de Giesen NC. 2012. De Saint-Venant equations-based model assessment in model predictive control of open channel flow. *Adv. Water Resour.* **49**:37–45.